IET Generation, Transmission & Distribution

Research Article

IET Journals
The Institution of Engineering and Technology

Impact of optimum power factor of PV-controlled inverter on the aging and cost-effectiveness of oil-filled transformer considering long-term characteristics

ISSN 1751-8687
Received on 15th March 2019
Revised 11th June 2019
Accepted on 24th June 2019
E-First on 26th July 2019
doi: 10.1049/iet-gtd.2019.0409
www.ietdl.org

Mohamed M.M. Salama[1], Diaa-Eldin A. Mansour[2], Samir Mohamed Abdelmakasoud[1], Ahmed A. Abbas[1]

✉

[1]*Department of Electrical Power and Machines Engineering, Benha University, Cairo, Egypt*
[2]*Department of Electrical Power and Machines Engineering, Tanta University, Tanta, Egypt*
✉ *E-mail: Ahmed_abdelmoneim@live.com*

Abstract: The photovoltaic (PV) system is one of the most widespread of the renewable energy generation systems that are being used to meet the continuously increasing energy demand. A proposed analytical method is used to find the optimum power factor of PV inverter (PVI) that leads to minimum aging, reduced energy losses cost of the transformer, lower payback period of PV system, and lower green houses gases (GHG) emissions due to the transformer energy losses. In this study, the thermal performance of a 630 kVA mineral oil-filled transformer is simulated in MATLAB programming language. For an association, it is mandatory to connect a PV system to the grid to minimise the transformer loading. The PV output power is used to study the long-term impact of the solar irradiance on the transformer thermal performance. Also, the long-term climatic characteristics are considered. The ambient temperature surrounding the transformer is considered all day long. The load current profile was measured all day long. The results show the aging and cost-effectiveness of the transformer and the payback period of PV system and GHG emissions are a function of PVI power factor.

1 Introduction

Electrical energy generated by photovoltaic (PV) system is environmentally friendly as there are no greenhouse gas (GHG) emissions. PV is a widespread renewable energy which can be rooftop, ground mounted, or integrated to building façade. PV system can be grid connected or standalone system to generate energy during daytime [1]. The grid-connected PV is a connection of PV system to the point of common coupling (PCC) at the transformer secondary side. In [2], the authors defined the optimum design and operation of PV grid connected system by minimising the payback period.

PV system generates the power in the DC form and the inverter is responsible to invert it to the AC form [3]. The operation of PV inverter (PVI) has an impact not only on the PV system itself but also on the entire system efficiency. The inverter operation can be adjusted to produce power at a certain power factor (PF) producing both active and reactive power [4]. In case of low penetration level of PV, the active and reactive powers will be injected to the load resulting in a reduction in transformer loading, loss of life, and losses. All these savings will reduce the payback period of the PV system. In case of high penetration level of PV, the surplus power of PV system than the load demand will be reversed and purchased by the utility. However, if this reverse power is higher than the transformer power rating, this will cause transformer overloading.

Several studies considered reactive power support of PV inverters, but only for the sake of low voltage ride-through capability. For high penetration level of PV, a sophisticated control strategy should be considered to meet the grid requirements [5–7]. In [8], the basis of the control scheme is the injection of the necessary reactive current to get back the voltage of PCC to the recommended limits by the utility. The PCC voltage, the inverter current, and the dc link voltage are used as inputs for the voltage controller. The output of the controller provides the related active power reference value to the necessary active power which should be injected to the grid. The inverter is connected to the PCC via LCL filter. LCL filter includes inverter side inductances, output side inductances, and filter capacitors.

In fact, various studies in the literature are targeting unity PF operation for PVI [9–11]. In [9], the authors utilised PVI at unity PF for the optimal design of secondary distribution system. Under normal operation, when PV inverter produces power at unity PF, this will reduce the active power before PCC causing a low PF fed by the transformer. The non-unity operation of PVI will reduce the active and reactive powers which are supplied via the transformer. In [12], the authors mentioned the availability of injection reactive power to get back the feeder PF before PCC. In [4], the efficiency of PVI is slightly reduced due to the additional losses for reactive power generation. The latest technologies of pulse width modulation (PWM) and high-frequency switching of semiconductors used in PVI led to high efficiency of conversion and low injection of harmonic distortion. As per the survey, PV grid connection inverters succeeded in achieving high conversion efficiency with keeping total harmonic distortion of current <5% [12, 13]. In [5], topologies have been mentioned for further improvement of the efficiency. In [8], a control scheme is presented to guarantee no harmonic distortion by injection reactive power. In [13], an LCL filter is included into PWM inverter to mitigate the high-frequency harmonics.

The internal heat generation inside the transformer is due to the total losses of the transformer which are the load losses and no-load losses. The load losses are the ohmic winding losses, winding eddy current losses, and other stray losses into the structural parts. This heat will be transferred to the ambient via the oil. Hence, the oil temperature and the winding temperature will be increased if the losses are increased [14]. Any increase in the oil temperature will accelerate its aging [15], and consequently, increase the transformer loss of life [9]. The transformer winding hottest spot temperature (HST) is the hottest temperature into the winding and its reference value is 110°C. If HST exceeded this thermal limit, the winding insulation will be deteriorated and causing the actual life-time is less than the normal lifetime. HST is a function of the loading current variation and the ambient temperature variation all day long. The transformer aging is a function of winding HST [9]. Hence, it is mandatory to study the impact of the different

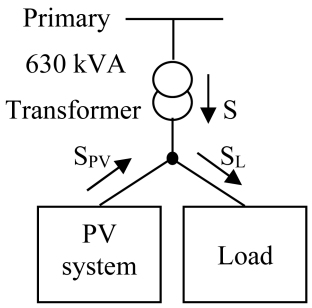

Fig. 1 *Grid connected PV system*

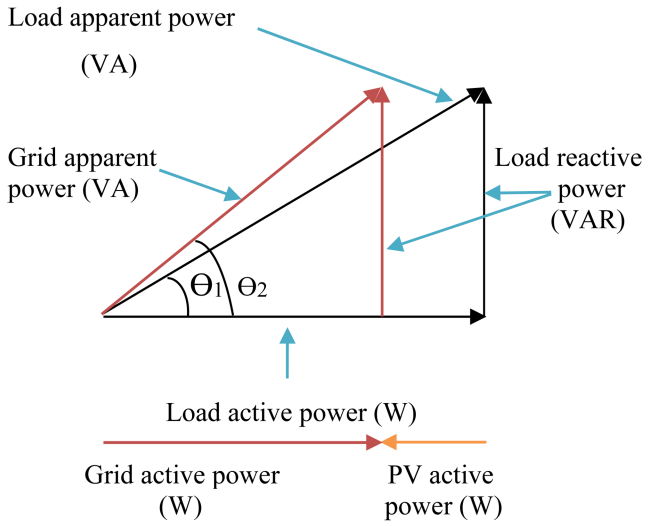

Fig. 2 *Power triangles of grid flow for no PV system and unity operation of PVI*

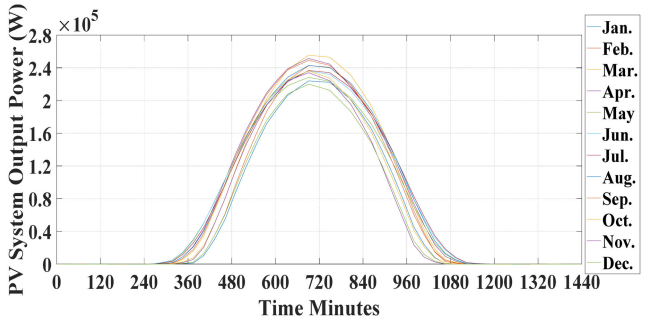

Fig. 3 *Daily PV system output power (W) at unity power factor as an average for the month*

scenarios of PVI PF to reduce the thermal stress and the loss of life of the transformer, which is the main aim of this study.

The main contribution of this paper is to investigate the aging and cost-effectiveness of oil-filled transformer used in grid-connected PV system considering the climatic conditions, such as temperature and solar irradiation, and operational conditions, such as loading and power factor. Based on this investigation, the optimum angle between the voltage and the current of PVI is adopted that will lead to minimising the transformer loss of life, reducing the transformer energy losses cost, and reducing the GHG emissions due to the transformer energy losses. This issue has not been studied elsewhere. The long-term ambient temperature and long-term solar irradiation are considered at Aswan, Egypt. The transformer energy losses due to the load losses depend on the transformer loading. The cost of the transformer energy losses are the energy losses (kWh) multiplied by the energy tariff (LE/kWh).

To achieve the abovementioned aims, three scenarios are proposed for this study. The first scenario is supplying the load without PV system. The second scenario is operating PVI at unity PF. As the penetration of PV system in this study is lower than the load demand, all active power will be provided to the load. The third scenario is to provide active and reactive powers by operating PVI at non-unity PF. Also for this scenario, the output of PV system is less than the load demand. Hence, all active and reactive powers will be provided to the load. Fig. 1 shows a 630 kVA, ONAN cooling type, and mineral oil-filled transformer, which is located at Aswan, Egypt, which feeds an association that needs to be equipped with PV system to minimise the consumed energy by the grid without increasing GHG emissions due to combustion of fossil fuels. The grid apparent power is abbreviated as S (VA), the load apparent power as S_{L} (VA), and the PV apparent power as S_{PV} (VA).

2 Grid-connected PV generation system

Our case study is on 630 kVA mineral oil transformer supplying an association that needs to be equipped with 270 kWp PV system. When PV system at unity power factor is connected to the grid, PV system injects active power only and reduces the grid active power flow to the load. This leads to increasing the angle between the voltage and the current of the grid from θ_1 to θ_2 and reducing the power factor as shown in Fig. 2. However when PV inverter produces leading angle between the current and the voltage, PV system injects active and reactive power and reducing the active and reactive power from the grid [2, 16]. In [17], the longitude and latitude axes for Aswan are 32.78°E and 23.97°N, respectively. The solar irradiance all year long at Aswan has been taken from [17]. The PV output at unity power factor is shown in Fig. 3 to study the impact of long-term characteristics at Aswan on the transformer aging and cost-effectiveness. The grid apparent power with PV system connected can be formulated as a function of PVI PF as follows:

$$S = \sqrt{(S_{\mathrm{L}}\cos\theta - S_{\mathrm{PV}}\cos\varphi)^2 + (S_{\mathrm{L}}\sin\theta - S_{\mathrm{PV}}\sin\varphi)^2} \tag{1}$$

where $\cos\theta$ is the load power factor, $\cos\varphi$ is the PVI power factor

The analytical method is based on the concept of derivation for the objective function of one variable and equals its derivative to zero for achieving the extremum theory. The point that causes the equality of the derivative is zero is called the optimum or the extremum point. Many forms can be utilised for analysing the optimisation problems. The minimisation of a function $f = f(\varphi)$ of one variable (φ) can be obtained, when the derivative of the function with respect to the variable (φ) is equal to zero. The value of the variable that will cause the derivative is equal to zero is called optimum value (τ) as given in (2) and (3) [18]

$$f'(\tau) = 0 \tag{2}$$

$$f(\varphi) \geq f(\tau) \quad \forall\varphi \tag{3}$$

The proposed analytical method is to differentiate the square of the transformer loading with respect to the angle (φ) between the voltage and the current of PVI. The value of (φ) that will cause the derivative is equal to zero is called the optimum angle. The objective function is a non-linear function of one variable which is the angle (φ) between the voltage and the current of the inverter. The optimum solution is the angle (φ) of PVI that minimises the transformer loading. The following analytical procedures are to find this optimum angle. From (1), the transformer loading will be reduced as follows:

$$S^2 = (S_{\mathrm{L}}\cos\theta - S_{\mathrm{PV}}\cos\varphi)^2 + (S_{\mathrm{L}}\sin\theta - S_{\mathrm{PV}}\sin\varphi)^2 \tag{4}$$

By differentiating (4) with respect to φ and equating the resultant to zero

$$\frac{\mathrm{d}S^2}{\mathrm{d}\varphi} = \sin(\theta - \varphi) = 0 \tag{5}$$

After differentiation, the resultant will be equating to zero

$$\varphi = \theta \tag{6}$$

The conclusion at the end of the analytical procedures is the necessity of the PVI to adjust the angle φ to be equal to θ for minimum transformer loading. At a certain time of the day ($t = 750$ min), the relation between the transformer loading and PVI angles (φ) is shown in Fig. 4. At this proposed time, the load apparent power (S_L) is 714 kVA, the angle (θ) is 32.33°, and the output apparent power of PV (S_{PV}) is variable all year long. At this proposed time and by substituting the values of S_L, θ, and S_{PV} in (4) and varying PVI angle (φ) with a wide range, it was found the transformer loading is a minimum when PVI angle (φ) is 32.33°. When the angle of the inverter increases from 0° to 32.33°, the transformer loading will decrease. Increasing PVI angle higher than 32.33°, the transformer loading will increase. Hence, for minimum transformer loading, the angle (φ) depends only on the angle (θ) not the solar radiation all year long. As the load PF is variable all day long, accordingly the PF of PVI will be variable all day long. The same load current into PU is considered for all months. Hence, for all months at the same time of the day ($t = 750$ min), the transformer loading will be minimum when the PVI angle (φ) is equal to 32.33°.

Impact of operation of PVI at non-unity PF on the efficiency of PVI and harmonics injection can be mitigated by utilising control schemes as in [5, 8]. The reduction into efficiency of PVI is not obvious due to the additional losses for reactive power injection to the grid. As the solar irradiance is changeable all day long, the efficiency of the proposed operation of PVI at optimum PF is changeable all day long with a minimum value of 98.45%. However, for unity operation of PVI, the efficiency is 98.6%.

The transformer loading was measured without connecting PV system and calculated that with connecting PV system at unity power factor as shown in Fig. 5. Fig. 6 shows the measured transformer loading without connecting PV system and the calculated transformer loading with considering PV inverter output at optimum power factor. In case of no PV system connection, PV output at unity PF, and PV output at optimum PF, the transformer was overloaded for a period of 615, 167, and 153 min respectively. However, the transformer maximum overloading values through these periods are 1.38, 1.29, and 1.26 pu, respectively, at instants of evening. Also in the case of no PV at instant of time ($t = 810$ min), the loading is 1.05 pu. Nevertheless, in the case of operation of PVI at unity and optimum PF, the loading is in range of 0.77–0.82 pu and 0.68–0.75 pu, respectively, for all months. Hence, the transformer loading capacity is increased in case of unity PF operation of PVI by 0.23–0.28 pu for all months. However that for optimum PF operation of PVI is increased by 0.3–0.37 pu all year long. The transformer thermal model is needed to monitor the winding HST to detect exactly if it is available to increase the capacity of the transformer or not. It may be noted the loading is less than the unity but the ambient temperature is high and the transformer is not capable to feed this load. Hence, the transformer thermal performance not only depends on the loading but also depends on the ambient temperature and the thermal parameters of the transformer.

3 Transformer thermal performance

Accurate thermal model is used to monitor the operating transformer winding HST. The accurate model will assist the utility to increase the transformer loading without exceeding the winding reference temperature value of 110°C and to reduce the unused capacity in the security margin [19]. The thermal–electrical analogy is used to apply the heat-transfer theory for simple and accurate calculation of the top oil temperature (TOT) and winding HST through transformer thermal model. This model considers the impact of the oil viscosity changes on the operating temperature. In this model, TOT model and HST model are two separate cascades interconnected considering changing thermal performance with the ambient temperature and the loading variations with time constant. The aging of the transformer is mainly dependent on the winding HST, which is the most crucial thermal parameter [20]. Fig. 7 shows the cascading interconnection for the transformer thermal models. The ambient temperature variation has a great impact on the transformer thermal performance especially for a hot region as

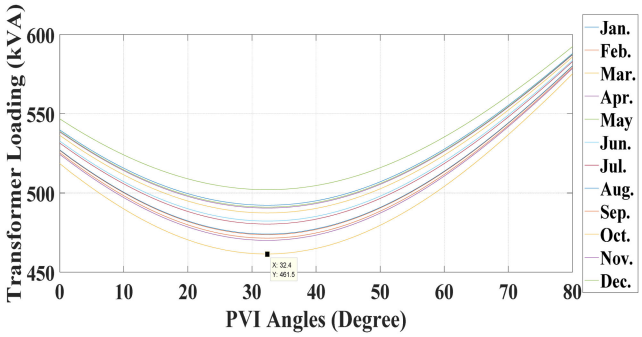

Fig. 4 *Transformer loading variation as a function of PVI angle (φ) at t = 750 min*

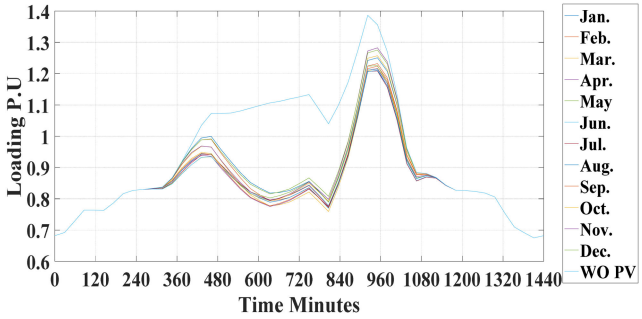

Fig. 5 *Transformer loading due to grid connected PV system at unity power factor and that without PV connection*

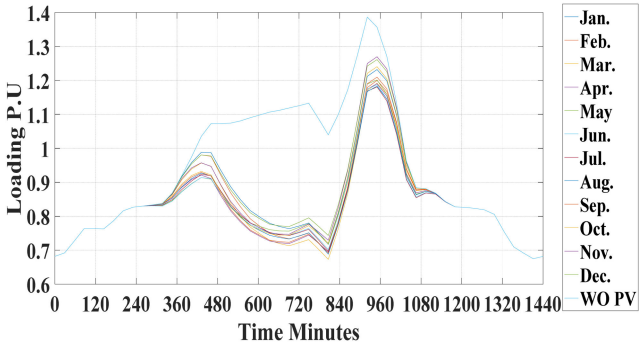

Fig. 6 *Transformer loading due to grid connected PV system at optimum power factor and that without PV connection*

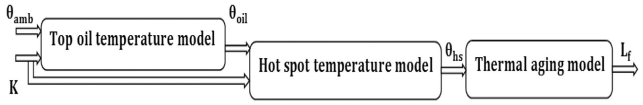

Fig. 7 *Transformer thermal model for loss of life calculation*

in Aswan. Fig. 8 shows the ambient temperatures all day long at Aswan as a month average. The daily ambient temperature of the coldest month (January) is in between 11 and 21°C and that of the warmest month (July) is between 27 and 40°C. A 630 kVA, ONAN cooling type, mineral oil-filled transformer has the thermal parameters as shown in Table 1. The thermal model exponents differ according to the cooling type as shown in Table 2.

3.1 Top oil temperature model

TOT can be simulated by IEEE top oil temperature rise model, improved top oil temperature model, or dynamic top oil thermal model. IEEE top oil temperature rise model proposed that if the ambient temperature changed, TOT will change instantly without oil time constant. Improved top oil temperature model enhanced the simulation of TOT and clarified TOT will change with ambient temperature with time constant. Dynamic top oil thermal model made another enhancement for TOT simulation and took into consideration the cooling type [19]. Nevertheless, Susa model

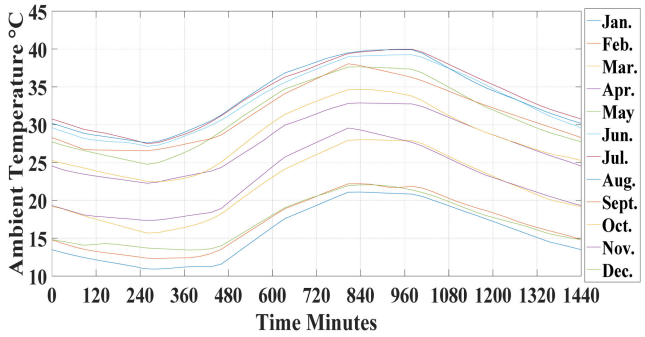

Fig. 8 *Ambient temperatures all day long at Aswan as a month average*

Table 1 Thermal parameters of 630 kVA mineral oil-filled transformer

Transformer parameters	Value
(I^2R) rated windings losses	9023 W
P_{EC-R} (rated windings eddy current losses)	665 W
P_{OSL-R} (other stray losses under rated conditions)	1350 W
no load loss	1195 W
PU eddy current losses at the hot spot location	0.72
ratio of rated load losses to no load losses	9.24
rated top oil rise	47.9°C
rated hot spot rise	23°C
exponent n	0.25
exponent *n*′	0.25

Table 2 Thermal model exponents for cooling types [21]

Cooling types	*n*′	*n*
no external cooling	0.25	0.25
with external cooling	2	0.5

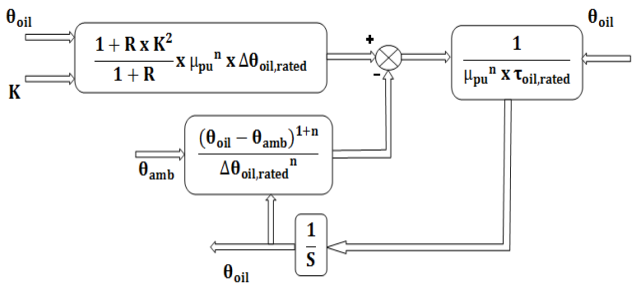

Fig. 9 *Block diagram of the top oil temperature model*

computes the transformer TOT considering the oil viscosity changes with the temperature. The increase in the transformer loading or the ambient temperature will lead to increasing TOT with time constant [20]. Fig. 9 shows the transformer top oil temperature model block diagram. The top oil temperature model is formulated as [22]

$$\frac{1+RxK^2}{1+R}x\mu_{pu}^{n}x\Delta\theta_{oil,rated}=\mu_{pu}^{n}x\tau_{oil,rated}x\frac{d\theta_{oil}}{dt}+\frac{(\theta_{oil}-\theta_{amb})^{1+n}}{\Delta\theta_{oil,rated}^{n}} \quad (7)$$

$$\tau_{oil,rated}=C_{th-oil,rated}\frac{\Delta\theta_{oil,rated}}{q_{tot,rated}}\times 60 \quad (8)$$

where $\Delta\theta_{oil,rated}$ is top-oil temperature under rated conditions rise over ambient (°C), θ_{oil} is operating temperature of the top-oil (°C), θ_{amb} is ambient temperature (°C), $\tau_{oil,rated}$ is time constant of oil under rated conditions (minutes), K is the specified load attribution to rated load, $q_{tot,rated}$ is transformer total losses under rated conditions (watt), R is attribution of rated load losses to no-load losses, μ_{pu} is per-unit oil viscosity, $C_{th-oil,rated}$ is oil thermal capacitance under rated conditions (J/°C) and n is the cooling constant for air moving fluid

The transformer oil thermal capacitance with external cooling is formulated as [20]

$$C_{th-oil}=Y_{wdn}\times m_{wdn}\times c_{wdn}+Y_{fe}\times m_{fe}\times c_{fe}+Y_{st}\times m_{mp}\times c_{mp}+O_{oil}\times m_{oil}\times c_{oil} \quad (9)$$

where Y_{wdn} is attribution of the winding losses to the total, losses of the transformer, Y_{fe} is attribution of the core losses to the total losses of the transformer, Y_{st} is attribution of the stray losses to the total losses of the transformer, m_{wdn} is winding material weight (kg), m_{fe} is core weight (kg), m_{mp} is tank and fittings weight (kg), m_{oil} is the oil weight (kg), c_{wdn} is winding material specific heat capacity ($c_{Cu}=0.11$ and $c_{Al}=0.25$ Wh/kg°C), c_{fe} is core specific heat capacity, ($c_{fe}=0.13$ Wh/kg°C), c_{mp} is tank and fitting specific heat capacity, ($c_{mp}=0.13$ Wh/kg°C), c_{oil} is the oil specific heat capacity, ($c_{oil}=0.51$ Wh/kg°C) and O_{oil} is the oil correction factor for the ONAF and OFAF cooling modes, ($O_{oil}=0.86$ Wh/kg°C),

The transformer oil thermal capacitance without external cooling is formulated as [21]

$$C_{th-oil}=m_{wdn}\times c_{wdn}+m_{fe}\times c_{fe}+m_{mp}\times c_{mp}+m_{oil}\times c_{oil} \quad (10)$$

Equation (7) is used to simulate TOT variations all day long for different scenario of PVI operation. Fig. 10 shows TOT variations all day long as an average for each month without connecting PV system. At a certain time of the day ($t=810$ min), TOT for all months is in between 74.8 and 90.1°C. In case of PV system output at unity PF, TOT for all months is in between 59.5 and 74.2°C as shown in Fig. 11. If PVI operates at optimum PF, TOT is in between 55.7 and 70.5°C for all months as shown in Fig. 12.

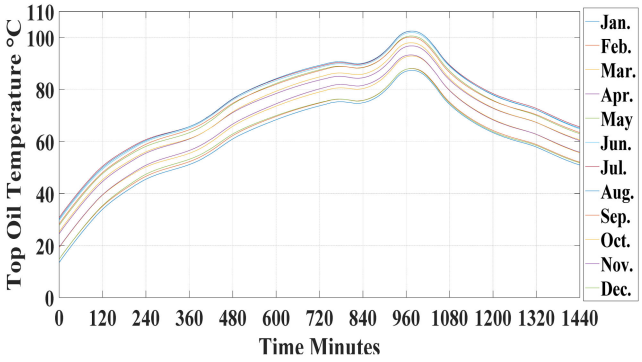

Fig. 10 *TOT without PV system*

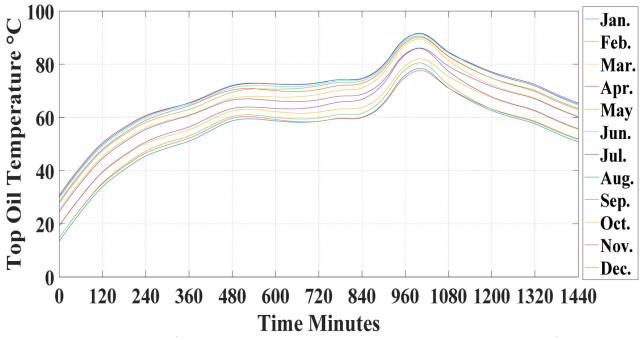

Fig. 11 *TOT for PV output power at unity power factor*

3.2 Winding hot spot temperature model

The winding temperature distribution is not homogenous and the hottest portion represents the winding hot spot temperature, which

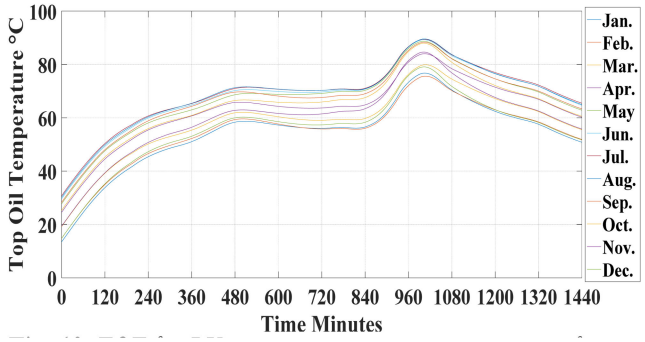

Fig. 12 *TOT for PV output power at optimum power factor*

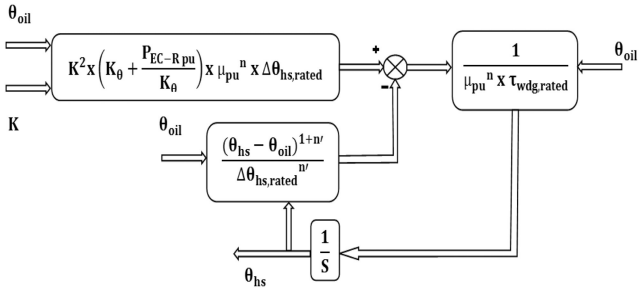

Fig. 13 *Block diagram of the hot spot temperature model*

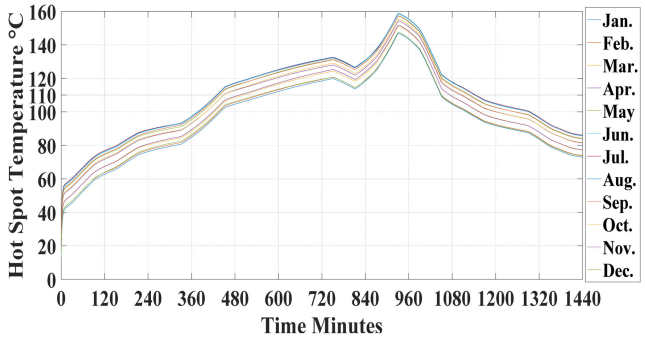

Fig. 14 *HST without PV system*

can damage the entire transformer or reduce its lifetime. Hence, it is the most crucial thermal parameter to determine the loading capability [23]. HST can be simulated by IEEE hot spot temperature rise model or dynamic hot spot thermal model. IEEE hot spot temperature rise model proposed that the winding HST will vary instantly with TOT without winding time constant. Dynamic hot spot thermal model took into consideration the cooling type for the simulation of HST [19]. However, Susa model considered the oil viscosity impact on the calculation of HST. The block diagram of HST model is shown in Fig. 13. The winding HST model is given as [22]

$$K^2 \times \left(K_\theta + \frac{P_{\mathrm{EC-R\,pu}}}{K_\theta}\right) \times \mu_{\mathrm{pu}}^{n} \times \Delta\theta_{\mathrm{hs,rated}} = \mu_{\mathrm{pu}}^{n} \times \tau_{\mathrm{wdg,rated}} \times \frac{\mathrm{d}\theta_{\mathrm{hs}}}{\mathrm{d}t} + \frac{(\theta_{\mathrm{hs}} - \theta_{\mathrm{oil}})^{1+n'}}{\Delta\theta_{\mathrm{hs,rated}}^{n'}} \tag{11}$$

$$K_\theta = \frac{\theta_K + \theta_{\mathrm{hs}}}{\theta_K + \theta_{\mathrm{avg}}} \tag{12}$$

where $P_{\mathrm{EC-R\,pu}}$ is pu winding eddy current losses under rated load and at hot spot location, $\Delta\theta_{\mathrm{hs,rated}}$ is hot spot temperature under rated conditions rise over top oil temperature (°C), θ_{hs} is operating temperature of winding hot spot (°C), $\tau_{\mathrm{wdg,\,rated}}$ is time constant of winding under rated conditions (minutes), $n'$is cooling constant for oil moving fluid, K_θ is resistance correction because of temperature

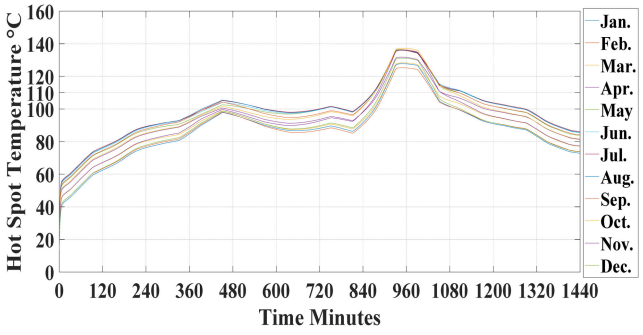

Fig. 15 *HST for PV output power at unity power factor*

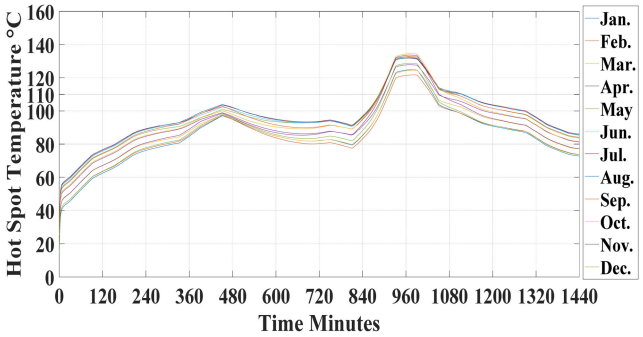

Fig. 16 *HST for PV output power at optimum power factor*

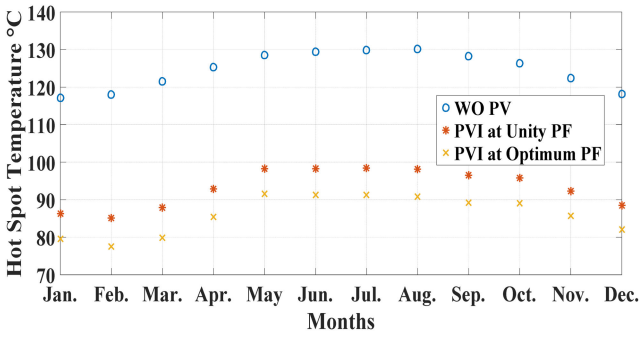

Fig. 17 *HST for PV output power at instant time (t = 810 min) in case of without connecting PV system, PV inverter at unity PF, and PV inverter at optimum PF*

change, θ_K is temperature factor for the loss correction, θ_{avg} is average winding temperature under rated load, $\theta_K = 235$ for copper, $\theta_K = 225$ for aluminium.

Equation (11) is used to simulate the winding HST in case of no PV system, PVI operation at unity PF, and optimum PF as shown in Figs. 14, 15 and Fig. 16, respectively. Fig. 17 shows HST at instant time ($t = 810$ min) for all months for the three cases. HST is in range between 117.1 and 130.2°C in case of no PV. When connecting PV system at unity PF to feed the power to the loads in conjunction with the utility, the winding HST reduced by 30.5°C in comparison with no PV. N in case of PVI operation at optimum PF, the winding HST is reduced by 38.5°C compared to NO PV system case.

4 Transformer aging

The preservation of the lifetime of the transformer plays a crucial role for the reliability of the power system. During the periods of the transformer overloading, the loss of life of the transformer increases as the winding HST exceeds the reference temperature value of 110°C. Aging acceleration factor (F_{AA}) is an indication factor for the aging of the transformer, which can be modelled as in (13). Through certain period of time dt, the loss of life (L_f) can be expressed as in (15) [23]

$$F_{\mathrm{AA}} = \mathrm{e}^{[(15,000/383) - (15,000/\theta_{\mathrm{H}} + 273)]} \tag{13}$$

$$dL = F_{AA}dt \tag{14}$$

$$L_f = \frac{1}{T}\int_0^T F_{AA}dt \tag{15}$$

$$L_f\% = \frac{\text{Accumulative age (hours)} * 100}{180,000} \tag{16}$$

From (13), if the winding HST is increased by 6.9°C, the transformer will lose half of its life as the aging acceleration factor will be doubled. Equation (16) is used to simulate the transformer loss of life for the three cases. The simulation of no PV system shows the daily loss of life percent is fluctuating from 0.0295 to 0.0887% according to the climatic and irradiance characteristics of each month as shown in Fig. 18. The sharpness of the loss of life curves in between 930 and 1000 min is due to the peak of the transformer loading and the ambient temperature at this period. Fig. 19 shows the daily loss of life has been reduced to be in between 0.0054 and 0.0157% for case of injection active power only from PV system. Fig. 20 shows the PV system injection at optimum power factor to the loads has been kept more reduction in the loss of life to be in between 0.0039 to 0.0121%. This means PVI operation at optimum PF has a great impact on the aging of the transformer.

5 Economic and environmental assessment

The economical aspects are necessary for engineers to make decisions involving the cost to choose one solution rather than another one. The engineers have a crucial role in making decisions based on the assessment of the expected outcome of the profitability analysis. Mathematical formulas are used for analysing and evaluating the engineering design alternatives [24]. The investment into the energy is in a continuous increase, so the energy losses cost need to be minimised to keep more profit for the investors. The utility and transformers users require more cost-effective transformer for economic aspects [25]. In this paper, the impact of connecting PV system at unity and non-unity power factor on the transformer cost-effectiveness is investigated referring to the case of no connected PV system. The bid price of the transformer is the same for the different cases of PVI operation, but the cost of transformer energy losses are dependent on the loading conditions. The considered loading conditions are function of the transformer thermal parameters, loading current, and the ambient temperature. The ambient temperature impact is based on the long-term conditions, so the cost-effectiveness is considered for each month. In [14], the load losses are expressed as shown in (18). The monthly energy losses are shown in Fig. 21. The current year cost of total energy losses of the transformer is expressed by summing the cost of the transformer energy losses for all months of the year as in (17). The monthly energy losses into the transformer are obtained by multiplying the daily energy losses into the transformer by the day per month and by the energy tarrif (LE/kWh). The daily energy losses (kWh) are obtained by integrating the total losses into the transformer (kW) all day long

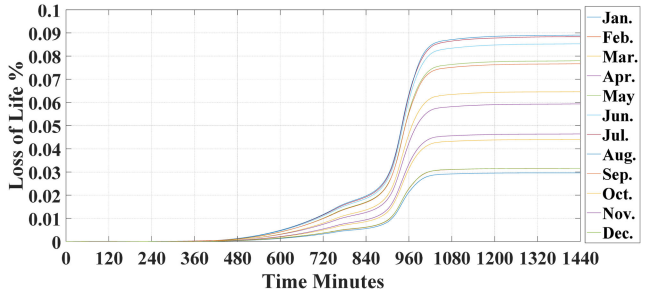

Fig. 18 *Daily loss of life percentage as an average for the month without PV system*

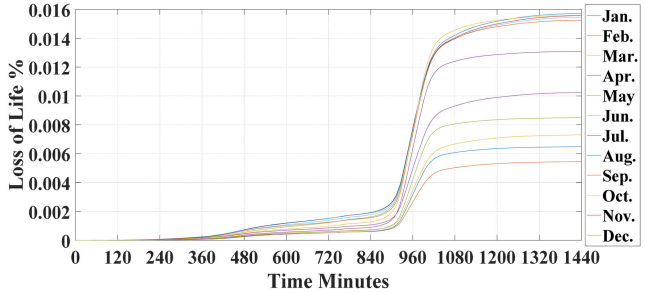

Fig. 19 *Daily loss of life percentage as an average for the month for PV output power at unity power factor*

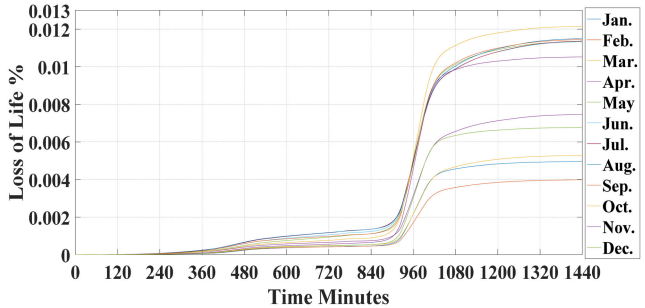

Fig. 20 *Daily loss of life percentage as an average for the month for PV output power at optimum power factor*

$$C_{TL} = \sum_{i=1}^{12}\left[DPM_i \times ET \times \int_0^T \left(NLL + LL \times K_i^2\right)dt\right] \tag{17}$$

$$LL = P \times K_\theta + \frac{P_{EC-R}}{K_\theta} + P_{OSL} \tag{18}$$

where C_{TL} is the annual cost (LE/year) of the transformer energy losses, NLL is no-load losses (kW), LL is rated load losses (kW), K_i^2 is the square of the specified load attribution to rated load for month i, P is ohmic losses (kW), P_{EC-R} is rated eddy current losses (kW), P_{OSL} is other stray losses (kW), ET is energy tariff (LE/kWh), DPM_i is days per month i (day), and i indicates the month.

The Egyptian average energy tariff is 1.05 LE/kWh. The payback period of the PV system can be obtained by dividing the total PV system cost by the saving of the consumed energy and energy losses costs. If the transformer particular rises with low losses, this will reduce the payback period. If the PVI operation led to more saving into the energy losses and the consumed energy, this will lead to more profit and low amortisation period. Also, the GHG due to combustion of fossil fuel for generation plants will be reduced. GHG emission can cost the authority to raise the health care. Hence, this cost is called environmental cost. When using the PF-controlled PVI through grid connection to minimise the transformer losses, the environmental cost is minimised.

For the environment protection, some countries set limit for the GHG emissions and the associations or utilities exceed this limit need to pay penalty or purchase GHG credits from other that have surplus of GHG credits. Hence, the environmental cost is included in the evaluation of the cost-effectiveness of the transformer. To evaluate the environmental cost due to the transformer energy losses, it is necessary to calculate the cost factor (LE/MWh) of the current year GHG emissions as follows: [26]

$$C = C_y \sum_{j=1}^{N} f_j \times e_j \tag{19}$$

$$e_j = \left(e_{CO_2,j} + 21e_{CH_4,j} + 310e_{N_2O,j}\right)\frac{0.0036}{n_j(1-\lambda_j)} \tag{20}$$

where C_y is cost of the current year GHG emissions (900 LE/t_{CO_2}), t_{CO_2} is equivalent tonnes of CO_2 emissions, j is fuel type, N is fuels number of electricity mixture, f_j is the percent of the consuming

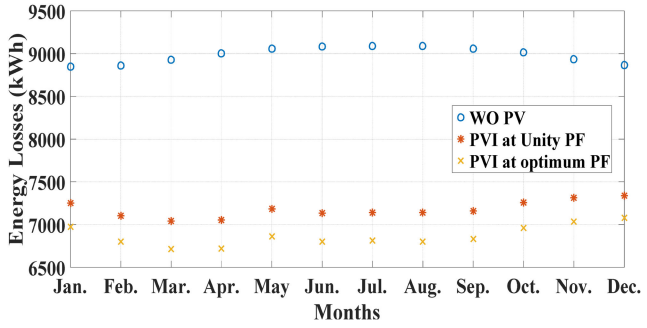

Fig. 21 *Monthly energy losses for case of without connecting PV system, PVI at unity PF, and PVI at optimum PF*

Table 3 GHG emissions of fossil fuel plants

Fuel type	Natural gas	Diesel	Coal
f_j, %	15	7.6	69.77
$e_{CO_2,j}$, kg/GJ	56.1	74.1	94.6
$e_{CH_4,j}$, kg/GJ	0.003	0.002	0.002
$e_{N_2O,j}$, kg/GJ	0.001	0.002	0.003
λ_j, %	8	8	8
n_j, %	45	30	35

Table 4 Annual energy losses, its cost, and its impact on the environmental cost

PVI status	WO PV	Unity PF of PVI	Optimum PF of PVI
annual energy losses, kWh	107,814	86,118	82,390
C_{TL}, LE/year	113,204.7	90,423.9	86,509.5
EC, LE/year	86,669.52	69,228.54	66,231.67
SEC, LE/year	—	17,440.98	20,437.85
t_{CO_2}	96.3	76.92	73.59

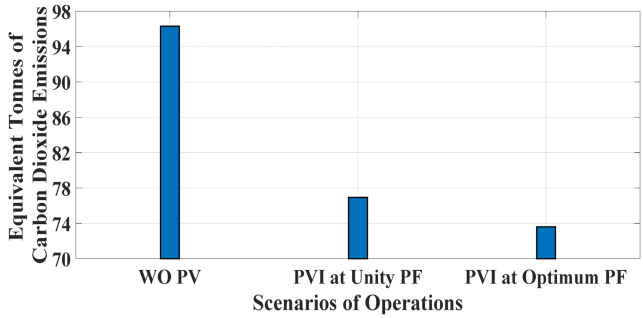

Fig. 22 *GHG emissions chart in case of without connecting PV system, PVI at unity PF, and PVI at optimum PF*

electricity coming from fuel j, e_j is the emission factor of fuel j (t_{CO_2}/MWh), $e_{CO_2,j}$ is emission factor of CO_2 for fuel j (kg/GJ), $e_{CH_4,j}$ is emission factor of CH_4 for fuel j (kg/GJ), $e_{N_2O,j}$ is emission factor of N_2O for fuel j (kg/GJ), λ_j is percent of energy lost in the grid for fuel j, and n_j is the conversion efficiency for fuel j (%)

To investigate the difference of the PVI operation impact on the environmental cost, the environmental parameters in [26] are considered. The considered emission GHGs are methane (CH_4), carbon dioxide (CO_2), and nitrous oxide (NO_2). Table 3 shows the considered fuel types. To determine GHG emissions due to transformer energy losses, the emission factor will be multiplied by the transformer energy losses.

The environmental cost is expressed by summing the monthly environmental cost due to the transformer energy losses as in (21). The monthly environmental cost due to the transformer energy losses is obtained by multiplying the day per month by the daily energy losses into the transformer and by the cost factor (LE/MWh) of the current year GHG emissions and by 0.001 to convert the cost factor to (LE/kWh). Also, the saving into the environmental cost due to the difference of the operation of PVI referring to the case of no PV is expressed by subtracting the annual cost of the environmental impact (LE/year) in case of operation of PVI at unity or optimum PF from that without PV as in (22)

$$\mathrm{EC} = \sum_{i=1}^{12}\left[\mathrm{DPM}_i \times C \times 10^{-3} \times \int_0^T \left(\mathrm{NLL} + \mathrm{LL} \times K_i^2\right)\mathrm{d}t\right] \quad (21)$$

$$\mathrm{SEC} = \sum_{i=1}^{12}\left[\mathrm{DPM}_i \times C \times \mathrm{LL} \times 10^{-3} \times \int_0^T \left(\Delta K_i^2\right)\mathrm{d}t\right] \quad (22)$$

where EC is the annual cost of the environmental impact (LE/year), SEC is saving into the annual cost of the environmental impact (LE/year), ΔK_i^2 is difference between the square of loading for month i.

The simulations show the annual energy losses of the transformer in case of unity PF of PVI is less than that without PV connection. However, in case of optimum PF of PVI, the energy losses are the minimum of the three scenarios as shown in Table 4. Hence, in case of optimum PF of PVI, the cost of the annual energy losses are the minimum. Also, the equivalent tonnes of CO_2 emissions are minimum due to the transformer energy losses are minimum and its environmental cost is the minimum. Fig. 22 shows a comparison chart of the equivalent tonnes of CO_2 emissions in case of without connecting PV system, PVI at unity PF, and PVI at optimum PF. The saving into the annual cost of the environmental impact is referring to the case of no PV. As well, the minimisation of the transformer energy losses is an indication for minimum amortisation period of the PV system. The payback period of PV system in case of unity PF of PVI is 11.3 year. Nevertheless that for optimum PF of PVI is 10.4 year referring to the case of no PV.

Now, the procedures of how to study the impact of PVI operation on the aging and cost-effectiveness of the transformer, the GHGs emissions, and the environmental cost are shown in Fig. 23.

6 Conclusions

The objective of this paper is to show the impact of PV power-factor-controlled inverter on the transformer loss of life, cost-effectiveness, GHG emissions, and environmental cost considering long-term characteristics of ambient temperatures and solar irradiance. It has been shown that the grid power factor is reduced when operating PVI at unity PF. However operating it at non-unity PF, this led to the improvement into the grid PF. A proposed analytical method is used to find the optimum PF of PVI to minimise the transformer loading. The transformer loading was measured in case of no PV system connection to the loads and was calculated in case of PVI operation at unity PF and optimum PF. These three scenarios of transformer loading are used to evaluate the impact of PVI operation. The considered transformer is 630 kVA, ONAN cooling type, and mineral oil. The top oil temperature and the winding hottest spot temperature are simulated for the three cases. The results show the operation of PVI to inject only active power leads to reducing HST by 30.5°C at time (t = 810 min) referring to no PV case. However the optimum PF of PVI leads to decreasing HST by 38.5°C at the same instant of time compared with no PV scenario. Also, the optimum PF minimised the daily loss of life to be in between 0.0039 and 0.0121% respecting to all months. The transformer energy losses are the minimum in between the three cases due to operating of PVI at optimum angle between the voltage and the current of the inverter. The minimisation of transformer energy losses led to minimising the GHGs emissions and also the environmental cost. Also, the payback period of PV system in case of unity PF of PVI is 11.3 year. However that for optimum PF of PVI is 10.4 year referring to

the case of no PV. Hence, PVI operation should be considered in the planning and design stage.

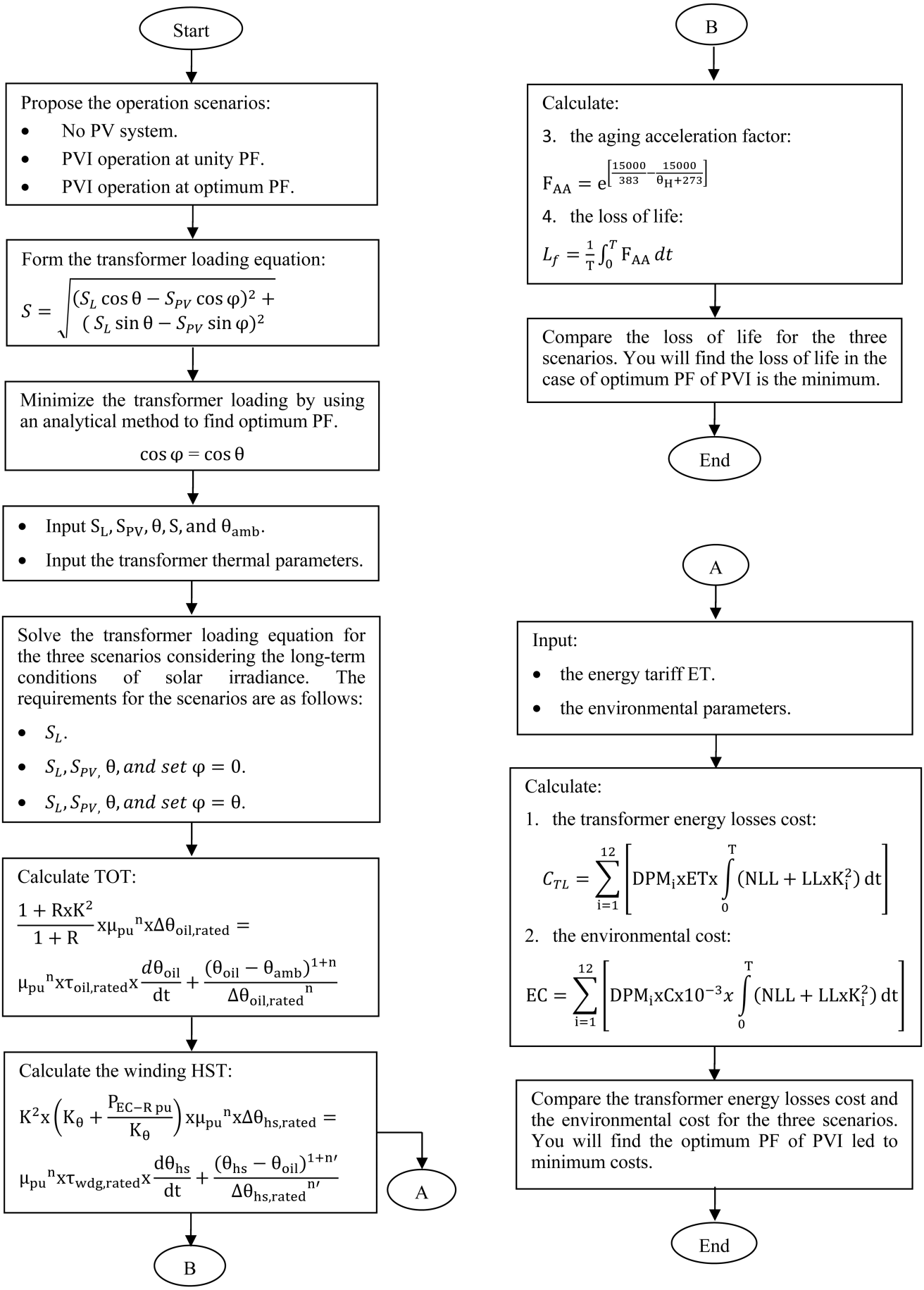

Fig. 23 *Procedures for the impact of PVI operation on the aging and cost-effectiveness of the transformer*

7 References

[1] Sehar, F., Pipattanasomporn, M., Rahman, S.: 'An energy management model to study energy and peak power savings from PV and storage in demand responsive buildings', *Appl. Energy J.*, 2016, **173**, pp. 406–417

[2] Hartner, M., Mayr, D., Kollmann, A., *et al.*: 'Optimal sizing of residential PV-systems from a household and social cost perspective – a case study in Austria', *Sol. Energy J.*, 2017, **141**, pp. 49–58

[3] Karimi, M., Mokhlis, H., Naidu, K., *et al.*: 'Photovoltaic penetration issues and impacts in distribution network – a review', *Renew. Sustain. Energy Rev. J.*, 2016, **53**, pp. 594–605

[4] Peng, W., Baghzouz, Y., Haddad, S.: 'Local load power factor correction by grid-interactive PV inverters'. 2013 IEEE Grenoble Conf., Grenoble, France, June 2013, pp. 1–6

[5] Yang, Y., Blaabjerg, F., Wang, H.: 'Low voltage ride-through of single-phase transformerless photovoltaic inverters', *IEEE Trans. Ind. Appl.*, 2014, **50**, pp. 1942–1952

[6] Brandao, D.I., Mendes, F.E.G., Ferreira, R.V., *et al.*: 'Active and reactive power injection strategies for three-phase four-wire inverters during symmetrical/asymmetrical voltage sags', *IEEE Trans. Ind. Appl.*, 2019, **1**, pp. 1–8

[7] Park, S., Kwon, M., Choi, S.: 'Reactive power P&O anti-islanding method for grid connected inverter with critical load', *IEEE Trans. Power Electron.*, 2018, **34**, pp. 204–212

[8] Miret, J., Camacho, A., Castilla, M., *et al.*: 'Control scheme with voltage support capability for distributed generation inverters under voltage sags', *IEEE Trans. Power Electron.*, 2013, **28**, pp. 5252–5262

[9] El Batawy, S.A., Morsi, W.G.: 'Optimal secondary distribution system design considering rooftop solar photovoltaics', *IEEE Trans. Sustain. Energy J.*, 2016, **7**, pp. 1662–1671

[10] Vu, P., Nguyen, Q., Tran, M., *et al.*: 'Adaptive backstepping approach for dc-side controllers of Z-source inverters in grid-tied PV system applications', *IET Power Electron.*, 2018, **11**, pp. 2346–2354

[11] Ma, L., Xu, H., Huang, A.Q., *et al.*: 'Single-phase hybrid-H6 transformerless PV grid-tied inverter', *IET Power Electron.*, 2018, **11**, pp. 2440–2449

[12] Eltawil, M.A., Zhao, Z.: 'Grid-connected photovoltaic power systems: technical and potential problems – a review', *Renew. Sust. Energy Rev.*, 2010, **14**, pp. 112–129

[13] Camacho, A., Castilla, M., Miret, J., *et al.*: 'Flexible voltage support control for three-phase distributed generation inverters under grid fault', *IEEE Trans. Ind. Electron.*, 2013, **60**, pp. 1429–1441

[14] Salama, M.M.M., Mansour, D.-E.A., Abdelkasoud, S.M., *et al.*: 'Impact of long-term climatic conditions on the ageing and cost-effectiveness of the oil-filled transformer'. 2018 Twentieth Int. Middle East Power Systems Conf. (MEPCON), Cairo, Egypt, 18–20 December 2018, pp. 494–499

[15] Emara, M.M., Mansour, D.A., Azmy, A.M.: 'Mitigating the impact of aging byproducts in transformer oil using TiO_2 nanofillers', *IEEE Trans. Dielectr. Electr. Insul.*, 2017, **24**, pp. 3471–3480

[16] Sreekanth, T., Lakshminarasamma, N., Mishra, M.K.: 'Grid tied single-stage inverter for low-voltage PV systems with reactive power control', *IET Power Electron.*, 2018, **11**, pp. 1766–1773

[17] https://sam.nrel.gov/weather, Monday, 3–9-2018, 11:00 am

[18] Serovajsky, S.: '*Optimization and differentiation*' (CRC Press, Boca Raton, FL, USA, 2018)

[19] Abbas, A., Elzahab, E.A., Elbendary, A.: 'Thermal modeling and ageing of transformer under harmonic currents'. 23rd Int. Conf. on Electricity Distribution, Lyon, France, 15–18 June 2015, pp. 1–5

[20] Susa, D., Nordman, H.: 'A simple model for calculating transformer hot-spot temperature', *IEEE Trans. Power Deliv.*, 2009, **24**, pp. 1257–1265

[21] Susa, D., Lehtonen, M.: 'Dynamic thermal modeling of power transformers: further development – part I', *IEEE Trans. Power Deliv.*, 2006, **21**, pp. 1961–1970

[22] Cui, Y., Ma, H., Saha, T., *et al.*: 'Moisture-dependent thermal modelling of power transformer', *IEEE Trans. Power Deliv.*, 2016, **31**, pp. 2140–2150

[23] Paterakis, N.G., Pappi, I.N., Erdinç, O., *et al.*: 'Consideration of the impacts of a smart neighborhood load on transformer aging', *IEEE Trans. Smart Grid*, 2016, **7**, pp. 2793–2802

[24] Blank, L., Tarquin, A.: '*Engineering economy*' (New York, USA, 2018, 8th edn.)

[25] Charalambous, C.A., Milidonis, A., Lazari, A., *et al.*: 'Loss evaluation and total ownership cost of power transformers – part I: a comprehensive method', *IEEE Trans. Power Deliv.*, 2013, **28**, pp. 1872–1880

[26] Georgilakis, P.S., Amoiralis, E.I.: 'Distribution transformer cost evaluation methodology incorporating environmental cost', *IET Gener. Transm. Distrib.*, 2010, **4**, pp. 861–872